Hyperbolic metamaterials based on multilayer graphene structures

Ivan V. Iorsh,[1,2] Ivan S. Mukhin,[1,3] Ilya V. Shadrivov,[4] Pavel A. Belov,[1,5] and Yuri S. Kivshar[1,4]

[1]*National Research University of Information Technologies, Mechanics and Optics (ITMO), St. Petersburg 197101, Russia*

[2]*Department of Physics, Durham University, DH1 3LE Durham, United Kingdom*

[3]*St. Petersburg Academic University, Nanotechnology Research and Education Center, St. Petersburg 194021, Russia*

[4]*Nonlinear Physics Center, Research School of Physics and Engineering, Australian National University, Canberra ACT 0200, Australia*

[5]*Queen Mary University of London, London E1 4NS, United Kingdom*

(Received 27 October 2012; revised manuscript received 13 December 2012; published 8 February 2013; corrected 10 July 2013)

We propose metamaterials for THz frequencies based on multilayer graphene structures. We calculate the dielectric permittivity tensor of the effective nonlocal medium with a periodic stack of graphene layers and demonstrate that tuning from elliptic to hyperbolic dispersion can be achieved with an external gate voltage. We reveal that such graphene structures can demonstrate a giant Purcell effect that can be used for boosting the THz emission in semiconductor devices. Tunability of these structures can be enhanced further with an external magnetic field which leads to the unconventional hybridization of the TE and TM polarized waves.

DOI: 10.1103/PhysRevB.87.075416 PACS number(s): 42.70.−a, 42.79.−e, 73.20.Mf, 78.67.Bf

I. INTRODUCTION

A hyperbolic medium is a special class of indefinite media[1] described by the diagonal permittivity tensor with the principal components being of the opposite signs which results in a hyperbolic shape of the isofrequency contours.[2,3] Such media have a number of unique properties including negative refraction[1,4] and subwavelength imaging.[5] One of the possible realizations of hyperbolic media is a periodic metal-dielectric nanostructured metamaterial where the hyperbolic nature of the isofrequency curves appears due to the excitation of the near-field plasmon Bloch waves.[6,7] Hyperbolic metamaterials have been realized for optical, infrared, and microwave frequency ranges. Realization of the THz hyperbolic media could allow boosting of otherwise slow THz radiative transitions in semiconductor devices which would lead to the development of a new class of THz sources.

Graphene, a two-dimensional lattice of carbon atoms, exhibits a wide range of unique properties.[8–10] Surface plasmons excited in individual graphene sheets have been extensively studied, both theoretically[11–17] and experimentally.[18,19]

In this paper, we suggest a class of hyperbolic metamaterials where individual graphene sheets are separated by host dielectric slabs, as shown schematically in Fig. 1. It is easy to notice an analogy between a graphene sheet placed inside a dielectric medium and a thin metal waveguide embedded into a dielectric matrix, which also supports localized surface plasmon polaritons. Assuming this analogy, we may expect that a periodic lattice of the graphene sheets may behave like an effective hyperbolic medium due to the coupling between the surface plasmons localized at the individual graphene sheets.[20] Importantly, surface plasmons in graphene have low losses and strong localization in the THz region. Indeed, as we demonstrate below, a periodic structure of graphene layers creates *a special type of metamaterial* with strong nonlocal response and hyperbolic properties of its dispersion curves for TM-polarized waves in the THz frequency range and superior characteristics such as a giant Purcell effect and tunability by a gate voltage or magnetic field. Although hyperbolic metamaterial for the THz range can be realized by using conventional metal-dielectric structures, very large negative permittivity of metals together with significant absorption at THz frequencies significantly limit the increase of the radiation efficiency of the emitters placed in such structures.

It is important to mention that the periodic layered structure shown in Fig. 1 resembles a natural graphite which is known to exhibit many interesting properties in the ultraviolet frequency range.[21] However, in the case of graphite, the π orbitals of the carbon atoms in the individual graphene planes strongly overlap which results in the modification of the electron band structure and large nonradiative losses. In the metamaterials we suggest here the electronic structure of the graphene sheets remains unperturbed.

II. HOMOGENIZATION OF THE MULTILAYERED GRAPHENE STRUCTURE

We consider the structure shown in Fig. 1 composed of graphene layers separated by dielectric slabs. Recently a graphene based hyperlens has been proposed in Refs. 22 and 23. However, the structure considered in this paper resembles the wire medium metamaterial and our structure is similar rather to the mutlilayered metadielectric metamaterials. First, we employ the transfer-matrix approach and analyze the dispersion properties of electromagnetic waves for both polarizations. We describe a graphene sheet by macroscopic parameters as a conducting surface defined by the frequency-dependent conductivity $\sigma(\omega)$:[24,25]

$$\sigma = \frac{2ie^2}{\hbar\pi}\times\left[\frac{1}{\hbar\omega+i\Gamma}v_F\int pdp\frac{\partial f(p)}{\partial p} - v_F\int dp\frac{\hbar\omega+i\Gamma}{(\hbar\omega+i\Gamma)^2-4p^2v_F^2}[f(p)-f(-p)]\right]. \quad (1)$$

Here v_F is the Fermi velocity of electrons in graphene, and $f(p)$ is the Fermi-Dirac distribution function: $f(p) = \{\exp[(pv_F-\mu)/T]+1\}^{-1}$, where μ is the chemical potential, and T is the temperature. Γ is the the electron collision frequency in graphene, which we set equal to 0.5 meV. The chemical potential is equal to 44 meV.

Electromagnetic boundary conditions at the graphene plane can be written as a matrix $\hat{M}$ connecting the tangential

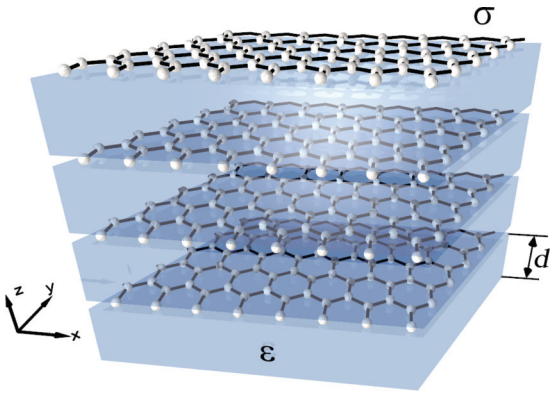

FIG. 1. (Color online) Geometry of the effective hyperbolic metamaterial composed of a periodic structure of graphene layers with conductivity σ separated by dielectric slabs with the thickness d and dielectric constant ϵ.

components of the electromagnetic field from both sides,

$$\hat{M}_{\mathrm{TE,TM}} = \begin{pmatrix} 1 & 0 \\ -4\pi\sigma/c & 1 \end{pmatrix}, \tag{2}$$

so that the transfer matrix for the structure period can be defined as $\hat{T} = \hat{S}\hat{M}\hat{S}$, where the matrix $\hat{S}$ is the transfer matrix of a dielectric layer. Then, we obtain the dispersion relation for the Bloch waves in the metamaterial structure in the form $\cos(Kd) = (\hat{T}_{11} + \hat{T}_{22})/2$, i.e.,

$$TE: \quad \cos(Kd) = \cos(k_z d) - \frac{2i\pi\sigma k_0}{k_z c}\sin(k_z d), \tag{3}$$

$$TM: \quad \cos(Kd) = \cos(k_z d) - \frac{2i\pi\sigma k_z}{k_0 c\varepsilon}\sin(k_z d), \tag{4}$$

where $k_z = (\varepsilon k_0^2 - \beta^2)^{1/2}$, β is the wave vector in the plane, K is the Bloch wave number, $k_0 = \omega/c$, and d is the period of the structure.

As is clear from Eqs. (3) and (4), the dispersion properties of the structure are defined by the graphene conductivity $\sigma(\omega)$ which depends on the chemical potential μ. Thus, changing μ with the external gate voltage we can tune the isofrequency contours of the metamaterial. For example, for the chemical potential $\mu = 44$ meV, the isofrequency curves of TM polarized waves are elliptic whereas they become hyperbolic for the gate voltage to 10 mV (see Fig. 2). The transition from the elliptical to hyperbolic regime has been studied recently in metamaterials,[26] and the graphene-based metamaterials offer a simple way for the realization of such transitions.

As has been established recently,[27] dispersion properties of nanostructured metal-dielectric metamaterials may demonstrate strong optical nonlocality due to excitation of surface plasmon polaritons, and these effects are more pronounced when the thicknesses of metal and dielectric layers are dissimilar. Accordingly, we expect graphene metamaterials to exhibit strong nonlocal properties having one of the layers vanishingly thin.

To derive the effective parameters characterizing the graphene metamaterial, we employ the nonlocal homogenization procedure.[28] Within this approach, we assume that the structure is excited with a harmonic external current

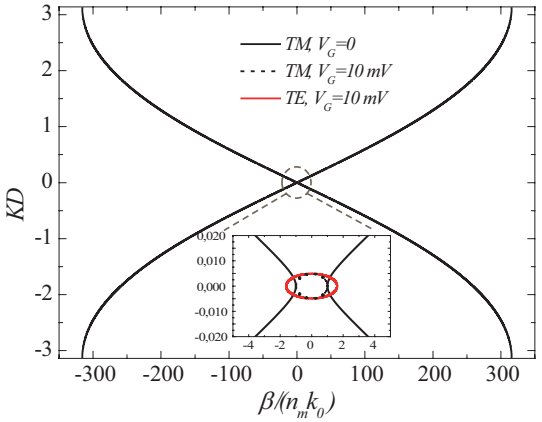

FIG. 2. (Color online) Isofrequency contours of the graphene metamaterial for the different values of the gate voltage and a fixed frequency of 4 meV.

$J \sim \exp[i(\beta x + Kz - \omega t)]$, and we calculate the electrical displacement averaged over the period of the structure.

After lengthy calculation employing the techniques from Ref. 28, we obtain the nonlocal dielectric permittivity tensor $\hat{\varepsilon}_{\mathrm{nloc}}$,

$$\hat{\varepsilon}_{\mathrm{nloc}} = \begin{pmatrix} \varepsilon_{xx} & 0 & 0 \\ 0 & \varepsilon_{yy} & 0 \\ 0 & 0 & \varepsilon_{zz} \end{pmatrix}, \tag{5}$$

with all nondiagonal elements vanishing and the remaining three components

$$\varepsilon_{xx} = \varepsilon - 2\alpha\left\{1 - 2\alpha\frac{k_z^2}{k_0^2}f(\beta,K)\right\}^{-1}, \tag{6}$$

$$\varepsilon_{yy} = \varepsilon - 2\alpha[1 - 2\alpha f(\beta,K)]^{-1}, \tag{7}$$

$$\varepsilon_{zz} = \varepsilon, \tag{8}$$

where $\alpha = 2\pi\,\mathrm{Im}(\sigma)/(k_0 dc)$, and the function $f(\beta,K)$ has the form

$$f(\beta,K) = \frac{k_0^2 d\sin(k_z d)}{2k_z[\cos(Kd) - \cos(k_z d)]} - \frac{k_0^2}{\left(k_z^2 - K^2\right)}. \tag{9}$$

For small values of β and K, the function $f(\beta,K)$ vanishes, and the components of the effective dielectric permittivity tensor become wave independent as in the case of quasistatic approximation and local media, $\varepsilon_{xx} = \varepsilon_{yy} = \varepsilon - 2\alpha$.

Figure 3(a) shows the dependence of the dielectric tensor component $\varepsilon_{xx} = \varepsilon - 2\alpha$ on the in-plane wave vector β for a fixed frequency of 40 meV, whereas the prediction of the local approach is shown with a straight dashed line. The component ε_{yy} deviates slightly from its local value $\epsilon - 2\alpha$, and it is not shown in the figure. We have used the value of $\varepsilon = 4$ for the dielectric permittivity of the host media, which is typical for the hexagonal boron-nitride (h-Bn)[29] being conventionally used in the multilayered graphene structure as a spacer due to its small lattice mismatch with graphene.

We observe that the nonlocal dielectric permittivity becomes negative for small values of βd. Because the component ε_{zz} is always positive, this results in a hyperbolic shape of

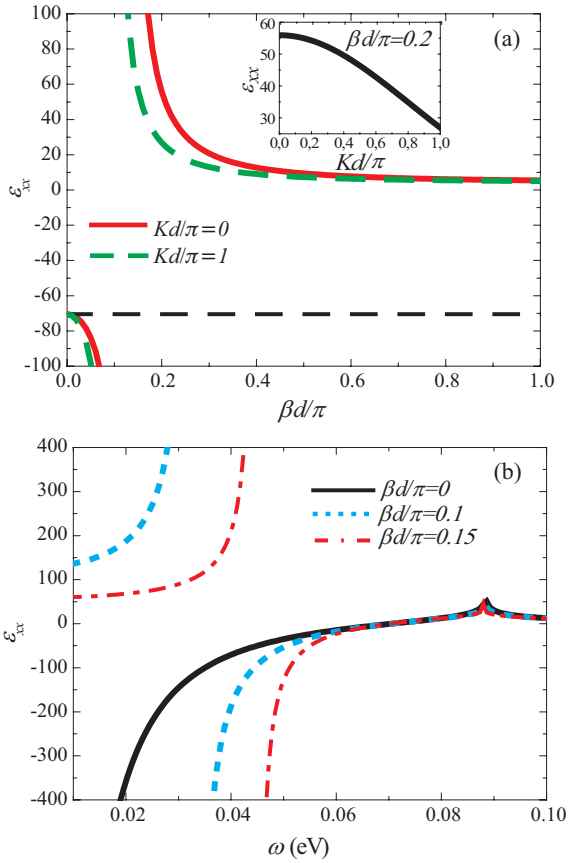

FIG. 3. (Color online) (a) Dependence of the component ε_{xx} on the in-plane wave vector β. Frequency is 40 meV; local approximation result is shown with a straight dashed line. Inset shows the dependence on K. (b) Frequency dependence of the component ε_{xx} for different values of β.

the isofrequency contours. However, for larger values of β the local approximation becomes invalid, and the component ε_{xx} changes its sign to positive, so an effective hyperbolic medium is transformed into elliptic one. This is a direct manifestation of strong nonlocal properties of the graphene metamaterials.

Figure 3(b) shows the dependence of the component ε_{xx} vs frequency. A solid line corresponds to the case of $\beta = 0$, and it coincides with the result of the local approximation. In this case, ε_{xx} may take very large negative values. However, there exist again strong discrepancies between local and nonlocal theories for the case of nonzero β. We observe that in this case there is a certain frequency corresponding to the pole of expression (8) for ε_{xx} below which the dielectric permittivity becomes positive.

III. CALCULATION OF THE PURCELL FACTOR

To illustrate some consequences of these results, we calculate the Purcell factor of a point dipole placed on top of the graphene metamaterial which characterizes the enhancement of the radiation efficiency as compared to the free space. In our structure we expect large Purcell factors for low frequencies. The expressions for the Purcell factors for both

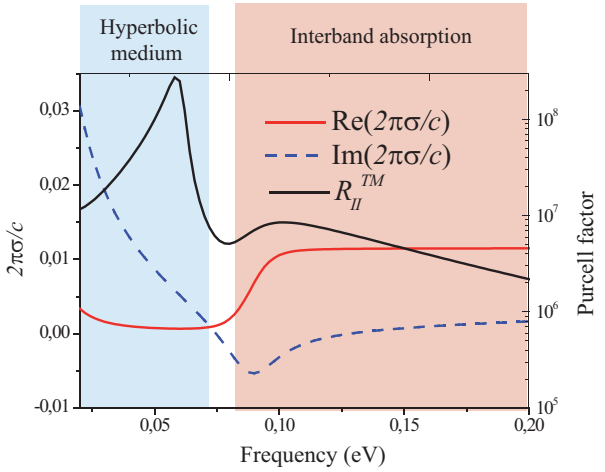

FIG. 4. (Color online) Purcell factor vs frequency for both TE and TM polarizations. Temperature is 4 K.

dipole orientations have the form[7]

$$R_{\parallel}^{TE} = \frac{3}{4}\mathrm{Re}\int_0^{\infty} \frac{\beta d\beta}{k_0\sqrt{k_0^2-\beta^2}} r_{TE}, \tag{10}$$

$$R_{\parallel}^{TM} = \frac{3}{4}\mathrm{Re}\int_0^{\infty} \frac{\beta\sqrt{k_0^2-\beta^2}d\beta}{k_0^3} r_{TM}, \tag{11}$$

$$R_{\perp}^{TM} = \frac{3}{4}\mathrm{Re}\int_0^{\infty} \frac{\beta^3 d\beta}{k_0^3\sqrt{k_0^2-\beta^2}}(-r_{TM}), \tag{12}$$

where signs $\parallel$ and $\perp$ correspond to the parallel and perpendicular orientations to the interface, respectively, and r_{TE},r_{TM} are the reflection coefficients from the semi-infinite layered structure. in the realistic graphene samples the collision rate Γ may vary from a couple of meV for the state of the art exfoliated graphene sheets to the tens of meV for the chemical vapor deposition (CVD) grown graphene sheets. In our calculations we use $\Gamma = 2$ meV. The Purcell factor is shown in Fig. 4 for the case of TM polarization. The Purcell factor for the TE case is close to unity in all the frequency range and is not shown. We observe that the low-frequency range is characterized by large Purcell factors for TM-polarized waves. This agrees with our observation of hyperbolic isofrequency contours for the low-frequency range in TM polarization. When we increase the frequency and move to the elliptic regime, the Purcell factor still remains significant which is connected with the large damping in the structure. Extraction of the radiation efficiency from the total Purcell factor is a main goal for future work. We also observe the increase of the Purcell factor at the frequencies close to the doubled chemical potential. This increase is connected with the additional damping due to the interband absorption which becomes significant at these frequencies, which results in the steplike increase of the real part of the conductivity. The steepness of the steplike increase of the real part of the conductivity is defined by the temperature. In order to minimize the nonradiative losses in the hyperbolic media region we should imply the condition $\mu/(k_B T) \ll 1$. In the THz frequency range, this condition corresponds to the temperatures of about 10 K.

We have also obtained analytical expressions for the $R_{\perp}^{TM}$ in two limiting cases. When the conductivity of graphene is small, the Purcell factor takes the form

$$R_{\parallel}^{TM} \approx \frac{3\pi\varepsilon^2}{2}\left(\frac{c}{2\pi|\mathrm{Im}(\sigma)|}\right)^3 \exp\left(-\frac{\varepsilon c k_0 d}{2\pi|\mathrm{Im}(\sigma)|}\right). \quad (13)$$

We notice that the Purcell factor is approaching zero exponentially when conductivity vanishes. When the conductivity is large, the expression for $R_{\perp}^{TM}$ reads

$$R_{\parallel}^{TM} \approx \frac{3\pi\varepsilon}{8(k_0 d)}\left(\frac{c}{2\pi|\mathrm{Im}(\sigma)|}\right)^2, \quad (14)$$

so that in the limit of infinite conductivity the Purcell factor vanishes.

Thus, the Purcell factor vanishes very large and very small conductivities. Thus, we should observe some maximum at the intermediate case. We have revealed that the maximum value of the Purcell factors is achieved for $\alpha = \varepsilon/2$. We notice that $\alpha = \varepsilon/2$ corresponds to *epsilon-near-zero metamaterial*. In this regime, the media is characterized by almost plane isofrequency contours and all evanescent modes can be excited.

In our calculations we did not account for nonlocal effects in graphene conductivity which should become significant for the in-plane vectors of the order of the Fermi wave vector: $k_F = \mu/v_F$, where v_F is the Fermi velocity of graphene electrons, and μ is the Fermi energy. We have checked how the nonlocality would modify the obtained results by performing integration in Eqs. (10)–(12) to k_F. We fix the frequency to 44 meV and change the period of the structure. We find that for small periods the effective model sufficiently overestimates the values of the Purcell factor. However, when the period is increased the values of the Purcell factors for both models are almost equivalent. We have also derived an analytical condition of good agreement between local model and the model which performs integration only over a finite range of wave vectors: $\coth[\mu d/(2v_F)] < 2\pi|\mathrm{Im}(\sigma)|\mu/(\omega v_F)$. A good agreement between local and nonlocal models allows us to expect strong THz radiation enhancement in multilayered graphene metamaterials.

IV. DISPERSION PROPERTIES OF THE METAMATERIAL IN STRONG MAGNETIC FIELD

We also study the properties of this metamaterial in the presence of a strong constant magnetic field. In this case, the surface conductivity of graphene is described by a 2×2 tensor with nondiagonal component equal to the Hall graphene conductivity σ_H. Furthermore, in the presence of strong magnetic field the longitudinal and Hall parts of the conductivities are governed by the electron transitions between the discrete Landau levels.[30] In addition, for the case of a single graphene sheet the magnetic field couples the TE and TM eigenmodes resulting in the emergence of new magnetoplasmonic eigenmodes.[31]

For the layered structure, we observe the similar coupling between the TE and TM modes. Indeed, the Bloch vectors of the system obey the following equation:

$$\cos(K_{1,2}d) = \frac{\mathcal{A}+\mathcal{B}}{2} \pm \sqrt{\frac{(\mathcal{A}-\mathcal{B})^2}{4} - \frac{\pi^2\sigma_H^2\sin^2(k_z d)}{\varepsilon}},$$
$$\mathcal{A} = \cos(k_z d) - \frac{2i\pi\sigma}{c}\frac{k_0}{k_z}\sin(k_z d), \quad (15)$$
$$\mathcal{B} = \cos(k_z d) - \frac{2i\pi\sigma}{c}\frac{k_z}{k_0\varepsilon}\sin(k_z d).$$

When the coupling term $\sim\sigma_H$ vanishes, Eq. (15) simplifies to Eqs. (3) and (4). In the presence of the magnetic field, the TE and TM polarized modes become coupled which results in complicated shapes of the isofrequency contours. To illustrate these results, we plot the eigenmodes isofrequency contours in the presence of constant magnetic field of 1 T applied along the z axis.

Figure 5(a) shows the dispersion of the longitudinal and Hall conductivities in the vicinity of the resonance corresponding to the transition between the zeroth and first Landau levels. Figure 5(b) shows the isofrequency contours of the electromagnetic eigenmodes at the frequency 100 meV. We observe that, although the imaginary part of the longitudinal conductivity is negative and we would expect the elliptic contours for both the eigenmodes, the coupling via the Hall

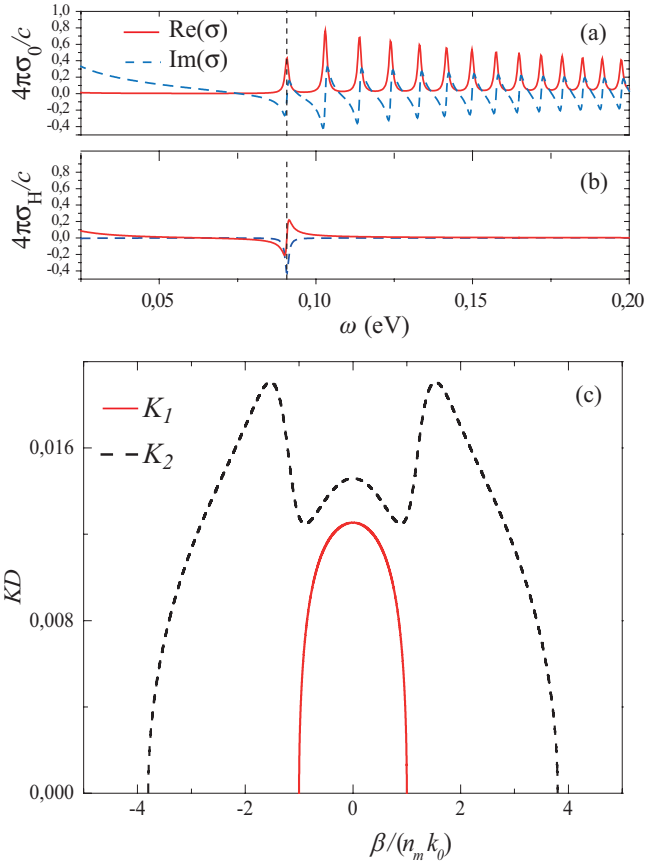

FIG. 5. (Color online) (a) Frequency dependence of the Hall and longitudinal conductivities in the presence of static magnetic field of 0.1 T. Temperature is 4 K. (b) Isofrequency contours for the frequency 100 meV for the first (red solid line) and second (blue dashed line) hybrid electromagnetic modes.

conductivity term changes the properties dramatically, and the isofrequency contours have a complicated shape, which is neither elliptical nor hyperbolic. The strong dependence of the isofrequency contours on the magnetic field suggests a different degree of freedom for engineering optical properties of these metamaterials.

V. DISCUSSION ON THE FEASIBILITY OF THE METAMATERIAL CONCEPT

Finally, we comment briefly on feasibility of the predicted effects. In our calculations we assume that the structure is infinite, and we apply Bloch's theorem. It is clear that experimentally only a limited number of periods can be manufactured. Similarly to photonic crystals, we expect that approximately ten periods should be sufficient in order for the multilayer structure to exhibit all major features of the band-gap material, and to observe the predicted effects. Our expectations are supported by the experiments with metal-dielectric nanostructures,[32] where ten-period metal-dielectric structures are shown to exhibit properties of the hyperbolic medium.

It is technologically achievable to make layered structures consisting of several graphene sheets separated by dielectric layers. For fabrication of single, double, and multiple graphene layers, or two-dimensional layers of other materials, the most popular approaches are cleavage technique[33] as well as CVD[34] and molecular beam epitaxy (MBE)[35] methods. There exist several methods of layer transfers, such as wet and dry transfer procedures with Poly(methyl methacrylate) (PMMA) and Polymethylglutarimide (PMGI), or water-soluble layer.[36–38] These methods retain a lot of residue after transfer, but the surface can be cleaned with Ar/H2 annealing. In a number of studies,[36–38] heterostructures composed of several graphene layers, boron nitride, or molybdenum flakes have been already demonstrated. Moreover, direct growth of graphene/h-Bn heterostructures by CVD methods[39] has also been demonstrated.

In this work, we have proposed of tunable graphene-based hyperbolic metamaterial, which can be controlled by an external voltage. In experiments, the voltage is provided by electrodes which could alter the structures response. As a possible solution, THz transparent dc conductors such as thin doped InSb films[40] can be employed as a host medium. These materials, however, exhibit THz transparency only under an applied magnetic field and in a narrow temperature range. On the other hand, if we use graphene/h-Bn heterostructure, h-Bn will limit the electrical tuning of the graphene sheets. The development of a realistic design of the structure that will allow optimal tuning is a subject of a separate work.

VI. CONCLUSIONS

In conclusion, we have demonstrated that a multilayer periodic structure composed of graphene layers can operate as a hyperbolic metamaterial in the THz frequency range, where tuning from elliptic to hyperbolic media can be achieved by applying an external gate voltage. We have predicted a giant Purcell effect for a point dipole source placed on top of such a metamaterial being achieved through coupling of effective plasmon modes with infinite wave numbers. We have also demonstrated a possibility of tuning the dispersion properties of the metamaterials with external magnetic field and the emergence of a family of hybrid eigenmodes in the graphene metamaterials.

ACKNOWLEDGMENTS

The authors thank the anonymous referees for the useful comments. This work was supported by the Ministry of Education and Science of Russian Federation (Grants No. 11.G34.31.0020, No. 14.B37.21.1649, and No. 14.B37.21.1941), the Dynasty Foundation, Russian Foundation for Basic Research (RFBR 12-02-12097), and the Australian Research Council.

[1] D. R. Smith and D. Schurig, Phys. Rev. Lett. **90**, 077405 (2003).
[2] H. Xie, P. Leung, and D. Tsai, Solid State Commun. **149**, 625 (2009).
[3] Z. Jacob, J. Kim, G. V. Naik, J. Kim, A. Boltasseva, E. E. Narimanov, and V. M. Shalaev, Appl. Phys. B **100**, 215 (2010).
[4] D. R. Smith, P. Kolinko, and D. Schurig, J. Opt. Soc. Am. B **21**, 1032 (2004).
[5] Z. Liu, H. Lee, Y. Xiong, C. Sun, and X. Zhang, Science **315**, 1686 (2007).
[6] A. P. Vinogradov, A. V. Dorofeenko, and I. A. Nechepurenko, Metamaterials **4**, 181 (2010).
[7] I. Iorsh, A. N. Poddubny, P. A. Belov, and Yu. S. Kivshar, Phys. Lett. A **376**, 185 (2012).
[8] R. R. Nair, P. Blake, A. N. Grigorenko, K. S. Novoselov, T. J. Booth, T. Stauber, N. M. R. Peres, and A. K. Geim, Science **320**, 1308 (2008).
[9] F. Bonaccorso, Z. Sun, T. Hasan, and A. C. Ferrari, Nat. Photon. **4**, 611 (2010).
[10] Q. Bao and K. P. Loh, ACS Nano **6**, 3677 (2012).
[11] S. A. Mikhailov and K. Ziegler, Phys. Rev. Lett. **99**, 016803 (2007).
[12] Yu. V. Bludov, M. I. Vasilevskiy, and N. M. R. Peres, Europhys. Lett. **92**, 68001 (2010).
[13] F. H. L. Koppens, D. E. Chang, and F. J. G. de Abajo, Nano Lett. **11**, 3370 (2011).
[14] M. Jablan, H. Buljan, and M. Soljacic, Opt. Express **19**, 11236 (2011).
[15] A. Y. Nikitin, F. Guinea, F. J. Garcia-Vidal, and L. Martin-Moreno, Phys. Rev. B **84**, 195446 (2011).
[16] A. Vakil and N. Engheta, Science **332**, 1291 (2011).
[17] B. E. Sernelius, Phys. Rev. B **85**, 195427 (2012).
[18] J. Chen, M. Badioli, P. Alonso-Gonzales, S. Thongrattanasiri, F. Huth, J. Osmond, M. Spasenovic, A. Centeno, A. Pesquera, P. Godignon, A. Z. Elorza, N. Camara, F. J. G. de Abajo, R. Hillenbrand, and F. H. L. Koppens, Nature (London) **487**, 77 (2012).
[19] Z. Fei, A. S. Rodin, G. O. Andreev, W. Bao, A. S. McLeod, M. Wagner, L. M. Zhang, Z. Zhao, G. Dominguez, M. Thiemens, M. M. Fogler, A. H. Castro-Neto, C. N. Lau, F. Keilmann, and D. N. Basov, Nature (London) **487**, 82 (2012).

[20]B. Wang, X. Zhang, F. J. García-Vidal, X. Yuan, and J. Teng, Phys. Rev. Lett. **109**, 073901 (2012).
[21]J. Sun, J. Zhou, B. Li, and F. Kang, Appl. Phys. Lett. **98**, 101901 (2011).
[22]A. Andryieuski, A. V. Lavrinenko, and D. N. Chigrin, Phys. Rev. B **86**, 121108 (2012).
[23]J. Wang, Y. Xu, H. Chen, and B. Zhang, J. Mater. Chem. **22**, 15863 (2012).
[24]L. A. Falkovsky and A. A. Varlamov, Eur. Phys. J. B **56**, 281 (2007).
[25]T. Stauber, N. M. R. Peres, and A. K. Geim, Phys. Rev. B **78**, 085432 (2008).
[26]H. N. S. Krishnamoorthy, Z. Jacob, E. Narimanov, I. Kretzschmar, and V. M. Menon, Science **336**, 205 (2012).
[27]A. A. Orlov, P. M. Voroshilov, P. A. Belov, and Yu. S. Kivshar, Phys. Rev. **84**, 045424 (2011).
[28]A. V. Chebykin, A. A. Orlov, A. V. Vozianova, S. I. Maslovski, Yu. S. Kivshar, and P. A. Belov, Phys. Rev. B **84**, 115438 (2011).
[29]A. F. Young, C. R. Dean, I. Meric, S. Sorgenfrei, H. Ren, K. Watanabe, T. Taniguchi, J. Hone, K. L. Shepard, and P. Kim, Phys. Rev. B **85**, 235458 (2012).
[30]V. P. Gusynin, S. G. Sharapov, and J. P. Carbotte, J. Phys.: Condens. Matter **19**, 026222 (2007).
[31]A. Ferreira, N. M. R. Peres, and A. H. Castro Neto, Phys. Rev. B **85**, 205426 (2012).
[32]T. Tumkur, G. Zhu, P. Black, Yu. A. Barnakov, C. E. Bonner, and M. A. Noginov, Appl. Phys. Lett. **99**, 151115 (2011).
[33]K. S. Novoselov, D. Jiang, F. Schedin, T. J. Booth, V. V. Khotkevich, S. V. Morozov, and A. K. Geim, Proc. Natl. Acad. Sci. USA **102**, 10451 (2005).
[34]N. Petrone, C. Dean, I. Meric, A. M. van der Zande, P. Y. Huang, L. Wang, D. Muller, K. L. Shepard, and J. Hone, Nano Lett. **12**, 2751 (2012).
[35]S. Godev, F. J. Ferrer, D. Vignaud, X. Wallart, J. Avila, M. C. Asensio, F. Bournel, and J. J. Gallet, Appl. Phys. Lett. **97**, 241907 (2010).
[36]K. S. Novoselov, A. K. Giem, S. V. Morozov, D. Jiang, S. V. Dubonos, I. V. Girgorieva, and A. A. Firsov, Science **306**, 666 (2004).
[37]C. Berger, Z. M. Song, T. B. Li, X. B. Li, A. Y. Ogbazghi, R. Feng, Z. T. Dai, A. N. Marchenkov, E. H. Conrad, P. N. First, and W. A. de Heer, J. Phys. Chem. B **108**, 19912 (2004).
[38]C. R. Dean, A. F. Young, I. Meric, C. Lee, L. Wang, S. Sorgenfrei, K. Watanabe, T. Taniguchi, P. Kim, K. L. Shepard, and J. Hone, Nat. Nanotechnol. **5**, 722 (2010).
[39]C. Bjelkevig, Z. Mi, J. Xiao, P. A. Dowben, L. Wang, W. N. Mei, and J. A. Kelber, J. Phys.: Condens. Matter **4**, 302002 (2010).
[40]X. Wang, A. A. Belyanin, S. A. Crooker, D. M. Mittleman, and J. Kono, Nat. Phys. **6**, 126 (2010).